Characterization and Control of Insulated Gate Interfaces on GaN-Based Heterostructures

Tamotsu Hashizume[1,2] and Masamichi Akazawa[1]

[1]Research Center for Integrated Quantum Electronics, Hokkaido University, Japan
[2]JST-CREST, Japan
e-mail: hashi@rciqe.hokudai.ac.jp

Keywords: GaN, AlGaN, MOS, interface, Al_2O_3, ALD

Abstract

We observed the peculiar capacitance-voltage (C–V) characteristics with two capacitance steps in the Al_2O_3/AlGaN/GaN structure prepared by atomic layer deposition. The detailed potential analysis showed that interface states near midgap or deeper in energies act as "fixed and frozen" charges at room temperature. From the voltage shift at the reverse bias in the photo-assisted C–V curve, we estimated the interface state density distribution at the Al_2O_3 /AlGaN interface for the first time.

Introduction

GaN-based high-electron-mobility transistors (HEMTs) are now applicable to next-generation switching devices, owing to a high blocking voltage and a low on-state resistance [1-8]. To realize a normally-off operation, a combination of recessed and insulated gates is often used in AlGaN/GaN HEMTs. To obtain stable and reliable recessed oxide gate structures, a low electronic state density at the Al_2O_3/AlGaN interface is absolutely required.

In comparison with a metal-oxide semiconductor (MOS) structure using a single semiconductor layer, it is very difficult to characterize oxide/AlGaN interfaces fabricated on AGaN/GaN heterostructures. They have two interfaces, making the potential modulation rather complex. In addition, the wide bandgap of $Al_xGa_{1-x}N$ (eg. 3.9 eV for x = 0.25) leads to an extremely low thermal emission rate of electrons at the interface states near the midgap or deeper energies. In this case, we cannot change the charge condition of such deeper states by bias sweeping in a standard capacitance-voltage (C-V) measurement at room temperature (RT). Accordingly, in this paper, we characterize the interface properties of the Al_2O_3 insulated gate on the AlGaN/GaN structure prepared by atomic layer deposition (ALD), especially focusing on the interface state density distribution by using a combination of standard and photo-assisted C–V measurements. Al_2O_3 is one of the attractive insulators for a gate structure applicable to FETs and HEMTs because of its high permittivity (8–10), bandgap (7–9eV) and breakdown field (>10MV/cm) values.

Experiments

The undoped $Al_{0.26}Ga_{0.74}N$/GaN heterostructure grown on a sapphire substrate by metal organic chemical vapor deposition was used in this work (provided by NTT-AT), as shown in Fig. 1. The sheet resistance and mobility of the AlGaN/GaN heterostructure were 480 Ω/sq. and 1550 cm^2/Vs, respectively.

We deposited a 10-nm-thick SiN film as a surface protection layer by electron-cyclotron resonance chemical vapor deposition, in order to avoid damage to the AlGaN surface during ohmic annealing [9]. As an ohmic electrode, a ring-shaped Ti/Al/Ti/Au (20/50/20/100 nm) multilayer structure was deposited on the AlGaN surface, followed by annealing at 800 ºC for 1 min in N_2 ambient. After the ohmic electrode process, the SiN layer was removed in a buffered HF solution. An Al_2O_3 film with a nominal thickness of 20 nm was then deposited on the AlGaN surface using an ALD system (SUGA-SAL100H) at 350 ºC for 170 cycles. In the ALD process, water vapor and trimethylaluminum were introduced into an ALD reactor in alternate pulse forms. The deposition rate of Al_2O_3 was 0.11 nm/cycle. Finally, a circular Ni/Au (20/50 nm) gate electrode was deposited on the Al_2O_3 layer.

Results and Discussion

1. C-V characteristics of Al_2O_3/AlGaN/GaN structure

Figure 2 shows the experimental C–V and G/ω–V curves of the 20-nm-Al_2O_3/AlGaN/GaN structure. We firstly carried out bias sweeping from 0 to -10 V. Then, the bias voltage was changed to the forward direction and swept to +6 V, and then back to 0 V. In the bias range

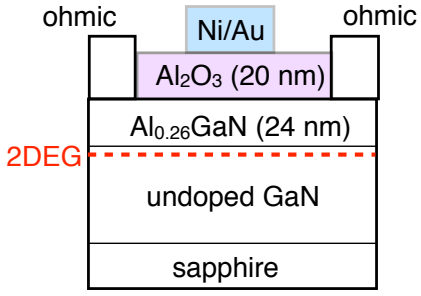

Fig. 1 Al_2O_3/AlGaN/GaN structure

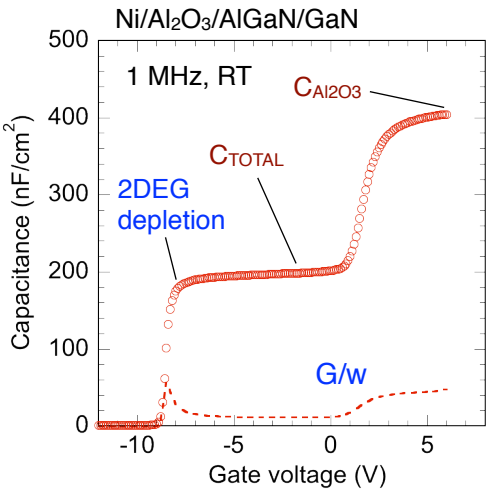

Fig. 2 Admittance characteristics of Al_2O_3/ AlGaN/GaN structure.

from -7 to 0 V, we observed an almost constant capacitance corresponding to the series capacitance of Al_2O_3 and AlGaN layers (C_{TOTAL}). In this bias region, the 2-dimensional electron gas (2DEG) exists with an almost constant density at the AlGaN/GaN interface. At around V_G= -9 V, a steep decrease in capacitance was observed, indicating the depletion of the 2DEG. At a forward bias of +1V, a steplike increase in capacitance occurred, reflecting the electron transfer from the AlGaN/GaN to the Al_2O_3/AlGaN interfaces.

To understand this C–V behavior, we calculated C–V curves and corresponding band diagrams, as shown in Figs. 3 and 4. The calculation was carried out using a numerical solver of the Poisson equation based on the one-dimensional Gummel algorithm, taking into account the fixed charge at the AlGaN/GaN interface originating from spontaneous and piezoelectric polarization as well as the charge in the electronic states at the Al_2O_3/AlGaN interface [10, 11]. We assumed two distributions of interface states with the minimum density of 1 x 10^{12} and 2 x 10^{12} cm^{-2} eV^{-1}, respectively.

All the calculated curves showed the two-step behavior, as observed in the experimental C–V result. Without the interface states, the C–V slope at step 1 is slightly steeper than that at step 2. However, this is not consistent with the experimental C–V curve (Fig. 2). The Al_2O_3/AlGaN interface in the actual structure includes electronic states. At around the forward bias near step 1, the nearly flat potential of the AlGaN layer shown in Fig. 4(a) can lead to the electron transfer from the AlGaN/GaN to Al_2O_3/AlGaN interfaces. However, at the same time, there is a high possibility of electron trapping at the Al_2O_3/AlGaN interface states. The acceptor-type states produce negative charges when they trap electrons. Such negatively charged interface states can screen the gate electric field, suppressing the potential modulation of the AlGaN layer. This causes the voltage shift at step 1 toward the positive bias direction, as shown in Fig. 3. In addition, the electron occupation rate of the interface states is a function of gate voltage (V_G), because the Fermi level (E_F) moves within the bandgap of AlGaN according to the V_G swing, as shown in Fig. 4(a). This also causes the stretch out (decrease) of the C–V slope. These characteristic features (voltage shift and stretch out of the C–V curve) are emphasized with an increase of the interface state density, as shown in Fig. 3.

On the other hand, the stretch-out behavior was not observed at step 2 in the experimental C–V curve (Fig. 2), which is consistent with the calculation result. Figure 4(b) shows a potential distribution at V_G = -8 V. In this bias region, the Fermi level is located far below the valence band maximum of AlGaN at the Al_2O_3/AlGaN interface.

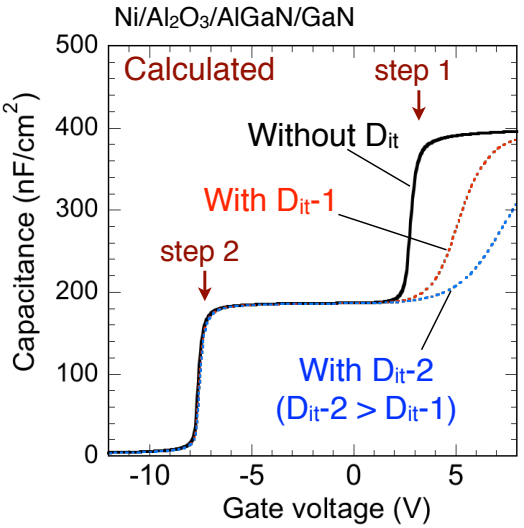

Fig. 3 Calculated C-V curves of Al_2O_3/AlGaN/ GaN structure.

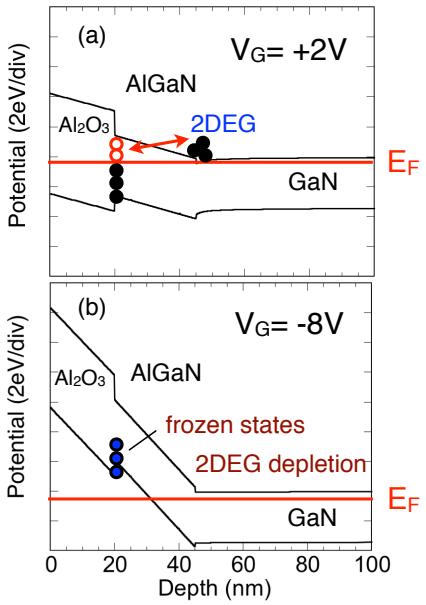

Fig. 4 Band diagram of Al_2O_3/AlGaN/ GaN structure.

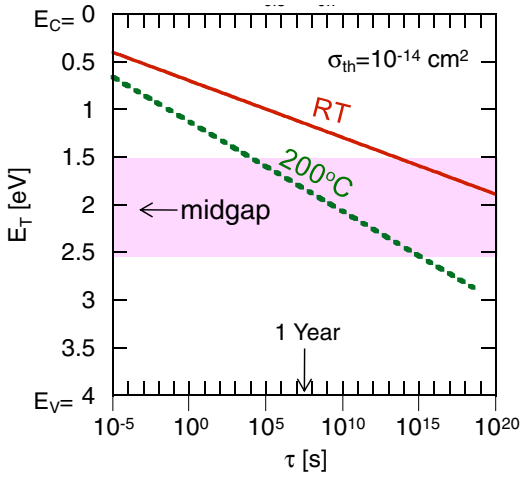

Fig. 5 Time constant τ for electron emission from the interface state to the conduction band of AlGaN as a function of .interface state energy E_T.

The electron occupation of interface states is no longer a function of V_G. In addition, an emission efficiency of electrons from the wide-gap interface states to the conduction band is very limited. The time constant of electron emission τ from interface states is given by Shockley-Read-Hall (SRH) statistics as follows.

$$\tau = \frac{1}{v_{TH}\sigma_{TH}N_C}\exp\left(\frac{E_T}{kT}\right) \qquad (1)$$

where v_{TH}, σ_{TH}, N_C and E_T are the electron thermal velocity, the capture cross section, the density of state at the conduction band, and the interface state energy, respectively. In the present case, as shown in Fig. 5, τ is estimated to be 10^{10}~10^{20} s for near-midgap states at room temperature (RT). Therefore, electrons captured at such deep interface states remain unchanged even when a large negative bias is applied to the gate electrode. This leads to the fact that the interface states act as "fixed and frozen" charges. Thus the stretch out of the C–V curve was not observed at step 2, and it is very difficult to detect interface states by a standard C-V measurement at RT.

2. Photoassisted C-V analysis

The photoassisted *C-V* measurement was performed to evaluate near-midgap electronic states at the Al_2O_3/AlGaN interface. First, we swept the gate voltage from +5 to -12 V under a dark condition. Then, the gate voltage was kept at -12 V and the monochromatic light (MAX-302, ASAHI Spectra) with a photon energy ($h\nu$) less than the bandgap of AlGaN was illuminated to the sample surface for 120 s. Consequently, we observed the photoassisted electron emission from the interface states with the energy range corresponding to the photon energy range, as schematically shown in Fig. 6. After the illumination, we restarted the *C-V* sweeping toward 0 V under a dark condition.

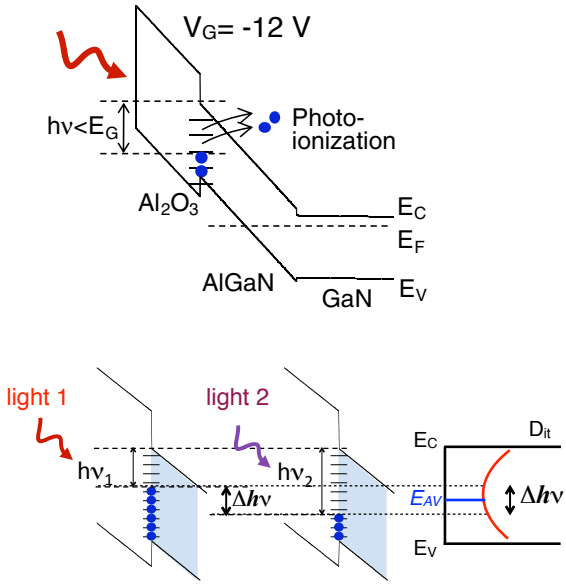

Fig. 6 Schematic illustration of photoassited C-V method.

Figure 7 shows the typical photoassisted *C-V* results. When the sample surface was illuminated with a higher photon energy, a larger amount of photoassisted electron emission causes larger V_{TH} shifts in *C-V* curves. The accurately parallel *C-V* shift toward the negative direction indicates that the interface states at Al_2O_3/AlGaN act as fixed charges in this bias range. The V_{TH} difference (ΔV_2) between two photon energies corresponds to the interface charge difference in the energy range from E_C - $h\nu_1$ to E_C - $h\nu_2$. To estimate the distribution of interface state density, the state density was calculated using the voltage difference ΔV_2 between two C–V curves with two photon energies by the following equation:

$$D_{it}(E = E_{AV}) = \frac{C_{TOTAL}\cdot\Delta V_2}{q\cdot\Delta h\nu} \qquad (2)$$

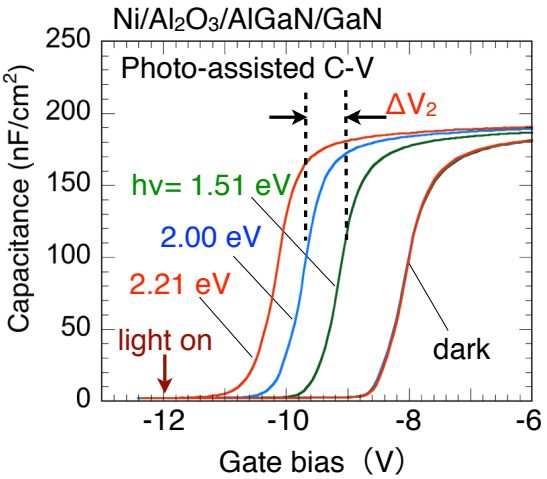

Fig. 7 Photoassited C-V characteristics of Al_2O_3/AlGaN/GaN structure.

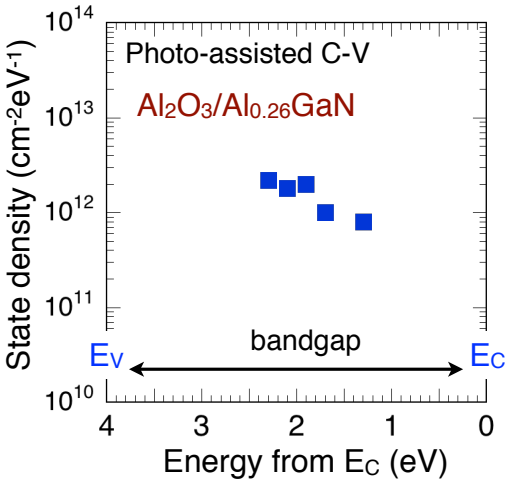

Fig. 8 State density distribution at the Al_2O_3/AlGaN interface determined by the photoassisted C-V analysis.

where C_{TOTAL} is the series capacitance of Al_2O_3 and AlGaN, Δhv is the difference between two photon energies, and E_{AV} is the average interface energy, as schematically shown in Fig. 6.

Figure 8 shows the interface state density distribution determined by the photioassisted C-V method. It was found that the Al_2O_3/AlGaN interface included interface states with densities higher than 1 x10^{12} $cm^{-2}eV^{-1}$. In comparison with the densities at the Al_2O_3/GaN interface [9], the present ALD-Al_2O_3/AlGaN interface has about one order of magnitude higher state density. The reason for this is not clear yet, but there is a possibility that the high interface state density is related to oxygen incorporation into the AlGaN or a high density of defect levels in the AlGaN layer [12, 13].

SUMMARY

We have characterized the interface properties of the Al_2O_3 insulated gate on the AlGaN/GaN structure prepared by ALD, especially focusing on the interface state density distribution at the Al_2O_3/GaN interface. The two capacitance steps were observed in the C–V curve in the Al_2O_3/AlGaN/GaN structure. The detailed potential analysis showed that interface states near midgap or deeper in energies act as "fixed and frozen" charges at RT. To evaluate near-midgap electronic states at the Al_2O_3/AlGaN interface, we have applied the photo-assisted C–V method to the heterostructure MOS samples. From the voltage shift at the reverse bias in the photo-assisted C–V curve, we estimated the interface state density distribution at the Al_2O_3 /AlGaN interface for the first time.

REFERENCES

[1] H. Kambayashi, Y. Satoh, S. Ootomo, T. Kokawa, T. Nomura, S. Kato, and T. P. Chow, Solid-State Electron. 54, 660 (2010).
[2] M. Kanamura, T. Ohki, T. Kikkawa, K. Imanishi, T. Imada, A. Yamada, and N. Hara, IEEE Electron Device Lett. 31, 189 (2010).
[3] H. Hahn, G. Lukens, N. Ketteniss, H. Kalisch, and A. Vescan, Appl. Phys. Exp. 4, 114102 (2011).
[4] R. Chu, A. Corrion, M. Chen, R. Li, D. Wong, D. Zehnder, B. Hughes, and K. Boutros, IEEE Electron Device Lett. 32, 632 (2011).
[5] A. Nakajima, Y. Sumida, M. H. Dhyani, H. Kawai, and E. M. S. Narayanan, IEEE Electron Device Lett. 32, 542 (2011).
[6] N. Otsuka, S. Nagai, H. Ishida, Y. Uemoto, T. Ueda, T. Tanaka, and D. Ueda, ECS Trans. 41, 51 (2011).
[7] D. Shibata, K. Kaibara, T. Murata, Y. Yamada, T. Morita, Y. Anda, M. Ishida, H. Ishida, T. Ueda, T. Tanaka, and D. Ueda, IEDM Tech. Dig., 26.2.1 (2011).
[8] M. Van Hove, S. Boulay, S. R. Bahl, S. Stoffels, X. Kang, D. Wellekens, K. Geens, A. Delabie, and S. Decoutere, IEEE Electron Device Lett. 33, 667 (2012).
[9] Y. Hori, C. Mizue, and T. Hashizume, Jpn. J. Appl. Phys. **49**, 080201 (2010).
[10] M. Miczek, C. Mizue, T. Hashizume, and B. Adamowicz, J. Appl. Phys. **103,** 104510 (2008).
[11] C. Mizue, Y. Hori, M. Miczek, and T. Hashizume, Jpn. J. Appl. Phys. **50,** 021001 (2011).
[12] K. Sugawara, J. Kotani and T. Hashizume, Appl. Phys. Lett. **94**, 152106 (2009).
[13] K. Ooyama, K. Sugawara, S. Okuzaki, H. Taketomi, H. Miyake, K. Hiramatsu, and T. Hashizume, Jpn. J. Appl. Phys. **49**, 101001 (2010).